Development of a bond-valence molecular-dynamics model for complex oxides

Young-Han Shin, Valentino R. Cooper, Ilya Grinberg, and Andrew M. Rappe*
Makineni Theoretical Laboratories, Department of Chemistry, University of Pennsylvania, Philadelphia, Pennsylvania 19104-6323, USA
(Received 19 July 2004; revised manuscript received 29 October 2004; published 11 February 2005)

A simple ten-parameter interatomic potential model is described that is capable of accurately reproducing the static and dynamical properties of complex oxides. The accuracy of this model stems from the crystal-chemical bond-valence theory of ionic and covalent bonding. The development of a specific variant of this model for ferroelectric $PbTiO_3$ (PT) is discussed in detail, and comparison of the model is made with density functional theory computations and with experimental data. Bond-valence molecular dynamics (BVMD) simulations for PT show a ferroelectric transition at 575 K. The BVMD model correctly reproduces the mixed order-disorder and displacive phase transition character, the magnitudes of cation displacements in the ferroelectric and paraelectric phases, and the energy of 180° domain walls. The success of this simple and physically motivated model makes the simulation of extended defects tractable in PT and other complex oxides.

DOI: 10.1103/PhysRevB.71.054104 PACS number(s): 77.84.−s, 77.80.Bh, 75.60.Ch, 31.15.Qg

Metal oxides exhibit useful mechanical, electrical, and magnetic properties that sensitively depend on the oxide stoichiometry and structure. Theory and computation can play valuable roles in revealing relationships between composition, structure, and properties. At the angstrom scale, quantum-mechanical modeling has elucidated many important aspects of oxide bonding. However, the development of multiscale models for oxides has proven difficult, due to the range of bonding interactions possible between various cations and oxygen. While important inroads have been made toward modeling larger regions of oxides (as described below), general-purpose tools for large-scale simulation of oxides are less developed than for other materials such as silicon and noble metals,[1–5] where 10^6-atom simulations are now tractable.

Since the complexity of oxide bonding is intimately related to the important properties, developing approaches for efficient oxide simulation is of significant fundamental and applied interest and has been addressed in several interesting ways. For ferroelectric perovskite oxides, the model Hamiltonian approach has proven most successful.[6,7] In this method, a subset of the degrees of freedom associated with important behavior (such as the ferroelectric phase transitions) is selected and fit to accurate quantum-mechanical calculations. Monte Carlo (or in some cases molecular-dynamics[8]) simulations can then be performed in this subspace, efficiently revealing salient features of complex oxides, such as the order of ferroelectric phase transitions with temperature[6] and composition.[9]

Despite these successes, there is still a strong need to develop a classical interatomic potential which accurately reproduces oxide properties. Model Hamiltonian approaches, because they focus on certain degrees of freedom, may not accurately capture the full range of behavior of the material, especially for configurations beyond the model training database. In addition, the selection of degrees of freedom to focus on requires significant insight into the material, retarding the development of such models for new systems. For these reasons, the straightforward creation of accurate classical potentials would accelerate understanding of oxides.

For ferroelectric perovskite oxides, the shell model and ReaxFF classical potentials have demonstrated success for bulk and thin-film *B*-site driven ferroelectrics $BaTiO_3$ and $KNbO_3$.[10–12] Recently, the development of classical models for the *A*-site- and *B*-site-driven ferroelectric $PbTiO_3$ (PT) has attracted great interest. PT has one of the highest known ferroelectric-to-paraelectric transition temperatures and is an end member of the technologically important solid solutions which are used in SONAR devices and in NVRAM memories. PT is perhaps the simplest Pb-based ferroelectric and a natural starting point for the development of the potentials for the more complicated solid solutions systems. Grinberg, Cooper, and Rappe demonstrated that a potential based on the bond-valence (BV) model accurately reproduced experimental and density functional theory (DFT) results for the structure of PZT solid solution.[13,14] Sepliarsky and Cohen have developed a shell model potential which reproduced the ferroelectric phase transition temperature.[15]

In this paper, we demonstrate a classical potential that can accurately reproduce the full dynamical behavior of PT, enabling the study of local structure changes accompanying phase transition and the examination of extended defects at finite temperature. To achieve this goal, we base the potential on the strong and simple physical principle of bond valence. In the bond-valence theory, the valence of an atom is assumed to be distributed among the bonds it forms, and the bond valences (or bond orders) are correlated with the bond length through an inverse power relation, with the total atomic valence of each atom equal to the sum of its bond valences. This approach to modeling the mixed ionic and covalent bonding in solids has been used to rationalize a wide variety of oxide crystal structures and was previously used to explain the local structure of the PZT solid solution.[13,14,16] Here, we use the BV formalism to treat Pb−O and Ti−O chemical bonding. The competition between the Coulombic and repulsive interactions has been shown to be important in governing ferroelectric distortions,[17] and we therefore include these two interactions in our potential. In addition, we introduce an angle potential to prevent unphysically large tilting of oxygen octahedra.

The total form of our potential E_{BV} is

$$E_{BV} = E_b + E_c + E_r + E_a, \tag{1}$$

where E_b, E_c, E_r, and E_a are the bond-valence potential energy, the Coulombic potential energy, the repulsive potential energy, and the angle potential energy, respectively. Following Brown's formulation[18] of the bond-valence theory, we define the bond-valence potential energy E_b as

$$E_b = \sum_{\beta=1}^{3} S_\beta \sum_{i=1}^{N_\beta} |V_{i\beta} - V_\beta|^{\alpha_\beta}, \tag{2}$$

where

$$V_{i\beta} = \sum_{\beta'=1}^{3} \sum_{i'(\mathrm{NN})} \left(\frac{r_0^{\beta\beta'}}{r_{ii'}^{\beta\beta'}} \right)^{C_{\beta\beta'}} \tag{3}$$

is the bond valence of the ith atom of type β. β is the index for Pb, Ti, and O ions, (NN) means the nearest-neighbor atoms, and N_β is the number of the β ions.[19] V_β is the desired atomic valence of the β ion, and $r_{ii'}^{\beta\beta'}$ is the distance between the ith β ion and the i'th β' ion. $r_0^{\beta\beta'}$ and $C_{\beta\beta'}$ are given from empirical values[20] and we set α_β to 1. Therefore, only S_β parameters need to be optimized in E_b. The repulsive potential energy E_r is defined as

$$E_r = \varepsilon \sum_{\beta=1}^{3} \sum_{i=1}^{N_\beta} \sum_{\beta'=1}^{3} \sum_{i'=1}^{N_{\beta'}} \left(\frac{B_{\beta\beta'}}{r_{ii'}^{\beta\beta'}} \right)^{12}, \tag{4}$$

where ε is the energy unit (1 eV) and the potential cutoff distance is 8 Å. $B_{\beta\beta'}$ are parameters to be optimized in Eq. (4). To correct the octahedral tilt at high temperature, we introduce the angle potential E_a,

$$E_a = k \sum_{i=1}^{N_{oct}} (\theta_{i,x}^2 + \theta_{i,y}^2 + \theta_{i,z}^2), \tag{5}$$

where k is the angle potential parameter to be optimized and N_{oct} is the number of the oxygen octahedra. $\theta_{i,x}$, $\theta_{i,y}$, and $\theta_{i,z}$ are the angles between the oxygen octahedral axes and the reference axes (e.g., $\theta_{i,x}$ is the angle between the x axis of the ith octahedron and the reference x axis[21]).

TABLE I. Optimized potential parameters of the bond-valence model potential function [Eqs. (1)–(5)]. The angle potential parameter k is 1.43 meV/(deg)^2.

			$B_{\beta\beta'}$ (Å)		
	q_β (e)[a]	S_β (eV)	Pb	Ti	O
Pb	1.554	0.236	—	2.311	1.741
Ti	0.739	0.175	—	—	1.287
O	−0.764	1.236	—	—	1.928

[a]Correspondingly, estimated charges with a Mulliken population analysis are 1.61e for Pb, 0.62e for Ti, and −0.74e for O (Ref. 23).

We used the simulated annealing global optimization method to find potential parameters that matched a database of DFT structural energy differences and atomic forces. The reference structures were obtained from *ab initio* density-functional-theory molecular-dynamics simulations within the local density approximation (LDA). We used the $2\times2\times1$ 20-atom supercell and 16 k points in the first Brillouin zone. DFT calculations were done with our in-house plane-wave code and Pb, Ti, and O pseudopotentials used in previous work.[22] The lattice constants a and c are 3.90 Å and 4.15 Å (c/a ratio=1.06). We constructed a database of 1770 reference structures at three different temperatures (10 K, 400 K, and 900 K) and selected 20 structures to be used in the fitting database. The fitted parameters (Table I) were validated by comparing the energies given by reference DFT calculations and BV model for all of the available DFT structures (Fig. 1), with excellent agreement obtained for a wide range of reference DFT structures absent from the fitting database. Our fitting procedure found that charges of 1.554e, 0.739e, and −0.764e for Pb, Ti, and O, respectively, gave the best agreement with DFT data (Table I). These charges are much smaller than the Born effective charges in PT as computed

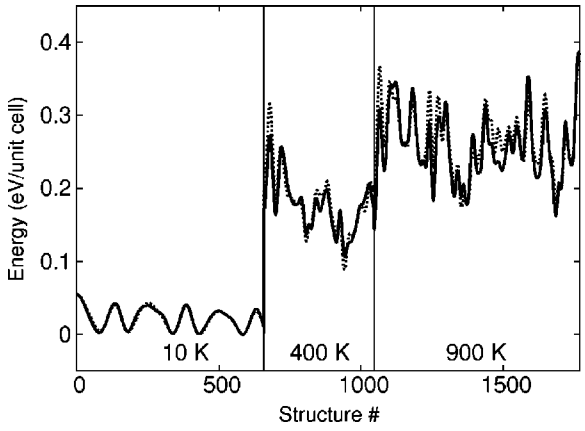

FIG. 1. Energy comparison between the *ab initio* result and the bond-valence model calculation using the optimized parameters in Table I. Solid lines represent the bond-valence model calculations, and dotted lines are DFT calculations.

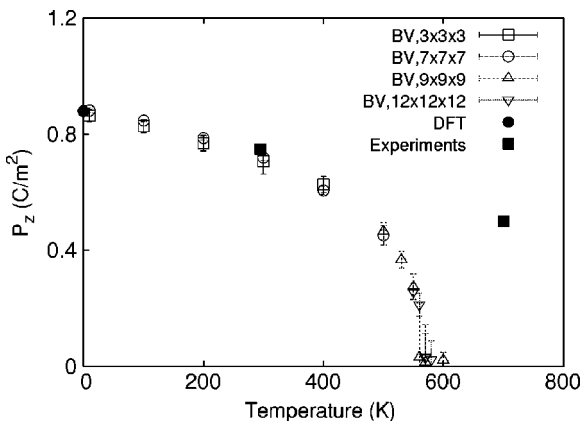

FIG. 2. The long-axis polarization P_z as a function of temperature shows the phase transition from the paraelectric structure to the ferroelectric structure. The experimental lattice parameters a and c were used at each temperature (Ref. 27), and experimental and DFT polarization data came from Refs. 29 and 30, respectively. The phase transition temperature converges to 575 K (the dotted line).

by our DFT calculations with the Berry-phase method and are similar to the Mulliken charges obtained for PT in a recent DFT study.[23] Such charges would give rise to much weaker dipole-dipole interactions between the individual unit cell dipoles. It is well known that the anomalous Born effective charges are due to the changes in covalent bonding with atomic motion. This effect is well characterized by our model, as most of the dipole-dipole interactions in PT are folded into the E_b term of our potential.

For initial validation of the model, we computed the ferroelectric instabilities (ΔE) and the 0-K Pb and Ti displacements for PT (Table II). To compare the energy well depth from the bond-valence model to the DFT value, we fixed the unit cell volume to 62.38 Å^3 and used two different c/a ratios (1.0 and 1.06). We find that BV calculations match DFT values very well, with differences of only ~20 meV and less than 0.06 Å error in ΔE and cation displacements, respectively.

We then applied our potential to finite-temperature molecular-dynamics (MD) simulations. The molecular-dynamics simulations were performed with the MOLDY code[25] modified to implement the nonadditive bond-valence model potential function. To avoid the known LDA errors for equilibrium perovskite volume,[26] we performed the simulation in the *NVT* ensemble at the experimental lattice constants[27] at each temperature using a Nosé-Hoover thermostat and time steps between 0.2 and 1.0 fs. The simulation size was varied from $3\times3\times3$ (135 atoms) to $12\times12\times12$ (8640 atoms).

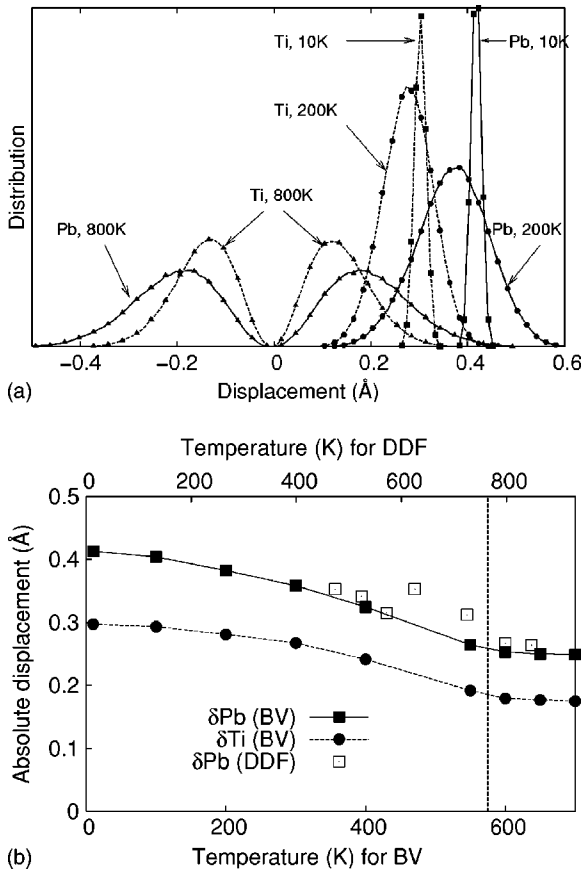

FIG. 3. Displacive and order-disorder characters in PT. At the paraelectric phase (800 K), it shows the order-disorder character (a), but this character is mixed with the displacive character at higher temperature (b). Pb displacement shows excellent agreement with the DDF result (Ref. 31) in the phase transition region.

TABLE II. Ferroelectric instabilities (energy well depths and displacements) and the domain wall energy (DWE) at 0 K.

	$c/a=1.0$		$c/a=1.06$	
	BVMD	DFT	BVMD	DFT
ΔE (eV)	0.080	0.063	0.142	0.160
δ_{Pb} (Å)	0.37	0.31	0.44	0.44
δ_{Ti} (Å)	0.26	0.20	0.30	0.28
DWE (mJ/m^2)	—	—	125	151 (132[a])

[a]Domain wall energy from Ref. 24.

To study the ferroelectric-to-paraelectric phase transition, we use the average polarization $\vec{P}$ as the order parameter, defined as the average of the local polarization $\vec{P}_l$:

$$\vec{P}_l = \frac{1}{V_u}\left(\frac{1}{8}\mathbf{Z}^*_{\mathrm{Pb}}\sum_{i=1}^{8}\vec{r}_{\mathrm{Pb},i} + \mathbf{Z}^*_{\mathrm{Ti}}\vec{r}_{\mathrm{Ti},i} + \frac{1}{2}\sum_{i=1}^{6}\mathbf{Z}^*_{\mathrm{O},i}\vec{r}_{\mathrm{O},i}\right), \quad (6)$$

where eight nearest-neighbor Pb atoms and six nearest-neighbor O atoms of a Ti atom are used for the calculation of the local polarization. $\mathbf{Z}^*_{\mathrm{Pb}}$, $\mathbf{Z}^*_{\mathrm{Ti}}$, and $\mathbf{Z}^*_{\mathrm{O}}$ are the Born effective charge tensors of Pb, Ti, and O computed by DFT calculations,[28] and V_u is the volume of the PT primitive unit cell. $\mathbf{Z}^*_{\mathrm{Pb}}$ and $\mathbf{Z}^*_{\mathrm{Ti}}$ effective charge tensors are diagonal and isotropic, and they were 3.66e and 6.40e for $\mathbf{Z}^*_{\mathrm{Pb}}$ and $\mathbf{Z}^*_{\mathrm{Ti}}$, respectively, in our DFT calculation. $\mathbf{Z}^*_{\mathrm{O}}$ is also diagonal but not isotropic. The element parallel to the cubic face is −2.40e and the element perpendicular to the cubic face is −5.26e. The evolution of $\vec{P}$ with temperature is shown in Fig. 2. We increased the cell size from $3\times3\times3$ to $12\times12\times12$ since the polarization in the transition region is sensitive to the size of the unit cell. As we increase MD cells to $12\times12\times12$, the phase transition temperature converges to 575 K.

For some years PT was thought of as an exemplary displacive ferroelectric. However, recent experiments revealed that the phase transition also has order-disorder character with Pb and Ti atoms locally displaced from the center of their oxygen cages even in the paraelectric phase.[31–33] In Fig. 3(a), we demonstrate the displacement distribution of Pb and Ti ions. At 10 K, Pb and Ti ions are displaced and their distributions are dense around 0.41 Å and 0.30 Å, respectively. As temperature increases to 200 K, displacements are slightly decreased and exhibit broader distributions. However, the displacive character still dominates over the order-disorder character at this temperature. At 800 K, the distributions are even broader, and the order-disorder character is now distinct. The mix of the displacive and order-disorder characters is shown in Fig. 3(b), where we compare the local displacement of Pb from the bond-valence model with the experimental distance distribution function (DDF) at various

temperatures.[31] In the phase transition region, Pb and Ti local displacements still remain and the trend of Pb displacement shows excellent agreement with the DDF result.

We further extended our model to the study of domain wall motion by calculating the energy of the 180° domain wall and comparing it to DFT results. The 180° domain wall separates an polarized-up domain from a polarized-down one, and the domain wall energy is the energy required to create a domain wall relative to the bulk energy in a unit area. The domain wall energies are shown in Table II for Pb-centered domain walls. For a $1\times10\times1$ simulation, the domain wall energy computed as the BV model was 125 mJ/m^2, in a good agreement with the DFT value of 151 mJ/m^2.

We applied the bond-valence model to the classical molecular-dynamics simulation of ferroelectric perovskites and compared the polarization, ferroelectric instability, and the domain wall energy from our model to the density functional calculation and the experimental data and found that our model potential reproduces those important physical quantities. Since the molecular-dynamics simulation with our model is fast enough for large systems, this model makes it possible to study the dynamics of ferroelectric domain wall motion and other extended defects. The accuracy of the empirical BV parameters for different types of oxides suggests that the bond-valence approach is promising for the creation of transferable atomic potentials. Finally, the simple physical meaning of each of the model parameters makes it possible to correlate atomic and solid state properties, providing fundamental insights into the physics underlying the excellent properties of the current materials as well as guidance for the search of new materials.

*Electronic address: rappe@sas.upenn.edu

[1] F. H. Stillinger and T. A. Weber, Phys. Rev. B **31**, 5262 (1985).
[2] M. Z. Bazant and E. Kaxiras, Phys. Rev. Lett. **77**, 4370 (1996).
[3] M. S. Daw and M. I. Baskes, Phys. Rev. B **29**, 6443 (1984).
[4] A. P. Sutton, M. W. Finnis, and D. G. Pettifor, J. Phys. C **21**, 35 (1988).
[5] R. E. Cohen, M. J. Mehl, and D. A. Papaconstantopoulos, Phys. Rev. B **50**, R14 694 (1994).
[6] W. Zhong, D. Vanderbilt, and K. M. Rabe, Phys. Rev. B **52**, 6301 (1995).
[7] U. V. Waghmare and K. M. Rabe, Phys. Rev. B **55**, 6161 (1997).
[8] H. Krakauer, R. Yu, C. Wang, and K. Rabe, J. Phys.: Condens. Matter **11**, 3779 (1999).
[9] L. Bellaiche, A. Garcia, and D. Vanderbilt, Phys. Rev. Lett. **84**, 5427 (2000).
[10] S. Tinte, M. G. Stachiotti, M. Sepliarsky, R. L. Migoni, and C. O. Rodriguez, J. Phys.: Condens. Matter **11**, 9679 (1999).
[11] M. Sepliarsky, S. R. Phillpot, D. Wolf, M. G. Stachiotti, and R. L. Migoni, J. Appl. Phys. **90**, 4509 (2001).
[12] W. A. Goddard, Q. S. Zhang, M. Uludogan, A. Strachan, and T. Cagin, in *Fundamental Physics of Ferroelectrics 2002*, edited by R. Cohen (American Institute of Physics, Melville, NY, 2002), pp. 45–55.
[13] I. Grinberg, V. R. Cooper, and A. M. Rappe, Nature (London) **419**, 909 (2002).
[14] I. Grinberg, V. R. Cooper, and A. M. Rappe, Phys. Rev. B **69**, 144118 (2004).
[15] M. Sepliarsky and R. E. Cohen, in *Fundamental Physics of Ferroelectrics 2002*, edited by R. Cohen (American Institute of Physics, Melville, NY, 2002), pp. 36–44.
[16] N. J. Ramer, E. J. Mele, and A. M. Rappe, Ferroelectrics **206**, 31 (1998).
[17] R. E. Cohen, Nature (London) **358**, 136 (1992).
[18] I. D. Brown, *Structure and Bonding in Crystals II* (Academic, New York, 1981).
[19] The cusp at $V_{i\beta}=V_\beta$ is numerically smoothed.
[20] For Pb–O, $C_{\beta\beta'}$ and $r_0^{\beta\beta'}$ are 5.5 and 2.044 Å and for Ti–O, 5.2 and 1.806 Å according to Ref. 18.
[21] $\theta_{i,x}$ is defined as $180\cos^{-1}(\hat{x}_r\cdot\hat{x}_i)/2\pi$, where $\hat{x}_r$ is the reference x axis, and $\hat{x}_i$ is the x axis of the ith octahedron.
[22] P. Juhas, I. Grinberg, A. M. Rappe, W. Dmowski, T. Egami, and P. K. Davies, Phys. Rev. B **69**, 214101 (2004).
[23] J. A. Rodriguez, A. Etxeberria, L. Gonzalez, and A. Maiti, J. Chem. Phys. **117**, 2699 (2002).
[24] B. Meyer and D. Vanderbilt, Phys. Rev. B **65**, 104111 (2002).
[25] MOLDY is developed by Keith Refson, and it is a free software following the terms of the GNU General Public License.
[26] Application of negative pressure, rescaling the temperature, or use of a different DFT exchange-correlation functional may also be used to fix this shortcoming.
[27] G. Shirane, S. Hoshino, and K. Suzuki, Phys. Rev. **80**, 1105 (1950).
[28] R. D. King-Smith and D. Vanderbilt, Phys. Rev. B **47**, R1651 (1993).
[29] V. G. Gavrilyachenko, R. I. Spinko, M. A. Martynen, and E. G. Fesenko, Sov. Phys. Solid State **12**, 1203 (1970).
[30] G. Sághi-Szabó, R. E. Cohen, and H. Krakauer, Phys. Rev. Lett. **80**, 4321 (1998).
[31] N. Sicron, B. Ravel, Y. Yacoby, E. A. Stern, F. Dogan, and J. J. Rehr, Phys. Rev. B **50**, 13 168 (1994).
[32] A. D. Bruce, K. A. Muller, and W. Berlinger, Phys. Rev. Lett. **42**, 185 (1979).
[33] N. Sicron, B. Ravel, Y. Yacoby, E. A. Stern, F. Dogan, and J. J. Rehr, Physica B **208**, 319 (1995).